Article

Discovery Medicine 2026; 38(208): 1597–1609
https://doi.org/10.24976/Discov.Med.202638208.125

Unveiling the Power of Astragaloside IV: A Novel Approach to Modulating KGN Cell Proliferation and Glycolysis Through the PPARγ/GNB2/PKM2 Axis

Wenchao Zhang[1], Shuzhen Zhang[1], Bin Wang[1], Jun Jiang[1], Mingxiao Wen[1,*]

[1]Department of Gynaecology and Obstetrics, The First Affiliated Hospital of Zhejiang Chinese Medical University (Zhejiang Provincial Hospital of Chinese Medicine), 310018 Hangzhou, Zhejiang, China

*Correspondence: wenmingxiao100@sina.com (Mingxiao Wen)

Submitted: 20 November 2025 Revised: 15 January 2026 Accepted: 26 January 2026 Published: 20 May 2026

Background: Polycystic ovarian syndrome (PCOS) is an endocrine disorder characterized by abnormal proliferation and apoptosis of ovarian granulosa cells (GCs), which contribute to follicular dysfunction and impaired ovulation. Although astragaloside IV (AS-IV) has shown anti-proliferative effects, its underlying mechanism remains unclear. This study aims to explore how AS-IV regulates the growth and apoptosis of human ovarian granulosa cell tumor (KGN) cells via glycolysis.

Methods: In this study, the human ovarian granulosa cell tumor line KGN was used as an *in vitro* model. AS-IV treatment was combined with genetic manipulations, including short hairpin RNA (shRNA)-mediated knockdown of G protein subunit beta 2 (GNB2) and overexpression of peroxisome proliferator-activated receptor gamma (PPARγ) and GNB2, to dissect their roles in AS-IV-mediated effects. The effects of AS-IV on KGN cell proliferation, apoptosis, lactate, pyruvate, and pyruvate kinase m2 (PKM2) levels via the PPARγ/GNB2 were evaluated. Chromatin immunoprecipitation and dual-luciferase reporter assays were used to study PPARγ's transcriptional regulation of GNB2. Ubiquitination and degradation of PKM2 by GNB2 were examined using immunoprecipitation.

Results: AS-IV induced apoptosis and lowered KGN cell growth ($p < 0.01$). Knockdown of GNB2 expression partially reversed the anti-proliferative and pro-apoptotic effects of AS-IV, indicating that GNB2 mediates AS-IV activity ($p < 0.05$). PPARγ transcriptionally regulated GNB2 expression, thereby enhancing the effect of AS-IV ($p < 0.05$). AS-IV upregulated the PPARγ/GNB2, inhibited PKM2 expression, and promoted PKM2 ubiquitination and degradation, further modulating glycolysis ($p < 0.05$).

Conclusion: This study reveals that AS-IV regulates KGN cell proliferation and apoptosis via the PPARγ/GNB2/PKM2 axis by inhibiting glycolysis. This study provides novel mechanistic insights into the therapeutic potential of AS-IV for PCOS by targeting granulosa cell metabolism and survival.

Keywords: granulosa cell; astragaloside IV; glycolysis; G protein subunit beta 2; peroxisome proliferator activated receptor gamma

Introduction

Polycystic ovary syndrome (PCOS) is a common endocrine and metabolic condition [1]. Its pathophysiology involves ovarian dysfunction, hormonal imbalances, insulin resistance, and chronic low-grade inflammation, with clinical manifestations varying between individuals [2]. PCOS is estimated at 8% to 13% in reproductive-aged women and 3% to 11% in adolescents, depending on the diagnostic criteria used and the population studied [3]. Current treatment approaches for PCOS encompass lifestyle modifications, pharmacological interventions, and assisted reproductive technologies [4–6]. The foundation of PCOS management is lifestyle modifications, including healthy dietary patterns and regular physical activity [7]. Pharmacologically, insulin sensitizers like metformin can alleviate insulin resistance, whereas oral contraceptives are frequently used to control menstrual periods and lower testosterone levels [8]. Anti-androgen medications may also be used to alleviate clinical symptoms in some patients [9]. However, the long-term efficacy of existing treatments remains suboptimal, with many patients experiencing disease recurrence or metabolic complications, highlighting the need for more precise and effective therapeutic strategies.

Astragaloside IV (AS-IV), a major active compound extracted from Astragalus membranaceus, possesses a broad range of pharmacological properties, including anti-inflammatory, antioxidant, immunoregulatory, and metabolic-improving effects [10]. AS-IV has shown substantial protective effects across diverse disease models, especially in metabolic disorders by enhancing energy metabolism, regulating insulin sensitivity, and demonstrating promise in the treatment of reproductive system diseases [11,12]. Because granulosa cells (GCs) are essential for follicular growth, maturation, and ovulation, their

dysfunction can result in the development of ovarian diseases [13]. In PCOS patients, abnormal GC proliferation is considered a key factor influencing follicular development [14]. In human ovarian granulosa cell tumor (KGN) cells and PCOS rat models, AS-IV controls the proliferation and death of ovarian tissue while simultaneously activating the Peroxisome proliferator-activated receptor gamma (PPARγ) [15]. Pyruvate kinase m2 (PKM2), a crucial rate-limiting enzyme in glycolysis that regulates energy metabolism and cell proliferation [16,17]. Therefore, the pathophysiology of PCOS may be significantly influenced by the PPARγ/PKM2 pathway. A recent study found that G protein subunit beta 2 (GNB2), the ubiquitin ligase of PKM2, plays an important role in cellular metabolic regulation [18]. In this study, we utilized the human granulosa cell tumor cell line (KGN cells) to explore the *in vitro* mechanisms by which AS-IV modulates GC proliferation and apoptosis. Our findings reveal that AS-IV influences glycolysis via the PPARγ/GNB2/PKM2, thereby regulating the proliferation and apoptosis of KGN cells.

Materials and Methods

Cell Culture

KGN cells (AW-CCH252, abiowell, Changchun, China), authenticated by short tandem repeat profiling, were cultivated in Dulbecco's Modified Eagle Medium (DMEM) (C0891, Beyotime, Shanghai, China) supplemented with 10% fetal bovine serum (FBS) (C0235, Beyotime, Shanghai, China). KGN cells, which can recapitulate disease-like phenotypes, are widely used as an *in vitro* model for simulating PCOS [19]. The cells were authenticated by short tandem repeat (STR) profiling and confirmed to be free of mycoplasma contamination.

Cell Transfection

Eight experimental groups were established from KGN cells: Control, short hairpin RNA negative control (shNC), shRNA targeting GNB2 (shGNB2)#1, shGNB2#2, shGNB2#3, negative control (NC), GNB2, and PPARγ. The short hairpin RNA (shRNA) and the controls were obtained from Yunzhou Biotechnology (Guangzhou, China); the overexpression plasmids and the controls were obtained from YouBio Biotechnology (Guangzhou, China) (Table 1). The coding sequence (CDS) region of PPARγ and GNB2 were provided in the **Supplementary Materials**. Before being transfected, KGN cells (5×10^5) were seeded in 6-well plates (FCP060, Beyotime, China) and incubated for the whole night. No therapy was given to the Control group. Cells were transfected with the corresponding 1 μg shRNA or 2 μg plasmid using Lipofectamine 2000 (11668019, Invitrogen, Carlsbad, CA, USA) according to the manufacturer's instructions. Western blot (WB) and reverse transcription-quantitative polymerase chain reaction (RT-qPCR) analyses were used to assess transfection effectiveness 48 hours after transfection.

Cell Grouping

Eight experimental groups were established from KGN cells: Control, AS-IV, AS-IV+shNC, AS-IV+shGNB2, AS-IV+NC, AS-IV+PPARγ, AS-IV+PPARγ+shNC, and AS-IV+PPARγ+shGNB2. The KGN cells in the AS-IV group were treated with 80 μg/mL AS-IV (HY-N0431, MCE, Monmouth Junction, NJ, USA) for 48 hours [20]. For the AS-IV+shNC, AS-IV+shGNB2, AS-IV+NC, AS-IV+PPARγ, AS-IV+PPARγ+shNC, and AS-IV+PPARγ+shGNB2 groups, after transfection with the respective shRNA and/or overexpression plasmids, cells were incubated with 80 μg/mL AS-IV for 48 hours.

Additionally, KGN cells were divided into four categories: Control, GNB2, Z-Leu-Leu-Leu-al (MG132), and GNB2+MG132. The GNB2 overexpression plasmid was transfected into KGN cells, then cultured for 48 hours in the GNB2 group. Subsequently, KGN cells were exposed to 10 μM MG-132 (HY-13259, MCE, Monmouth Junction, NJ, USA) for 6 hours in the MG132 group. KGN cells were transfected with the GNB2 overexpression plasmid and cultured for 48 hours before being treated with 10 μM MG-132 for 6 hours in the GNB2+MG132 group.

RT-qPCR

Total RNA was extracted from cells using TRIzol reagent (R0016, Beyotime, Shanghai, China) according to the manufacturer's instructions. Complementary DNA (cDNA) was synthesized using the Transcriptor First Strand cDNA Synthesis Kit (04379012001, Roche, CA, USA). SYBR Green PCR Master Mix (4344463, Thermo Fisher, Waltham, MA, USA) was applied in real-time PCR using an ABI 7500 real-time PCR machine (Applied Biosystems, Foster City, CA, USA) to assess gene expression. *β-actin* was employed as an internal control, and relative gene expression levels were calculated using the $2^{-\Delta\Delta Ct}$ method [21]. Primer sequences (Tsingke, Beijing, China) are listed in Table 2.

WB Analysis

Cells were lysed using radioimmunoprecipitation assay (RIPA) buffer containing protease inhibitors (P0013, Beyotime, Shanghai, China). The bicinchoninic acid (BCA) protein assay kit (P0009, Beyotime, Shanghai, China) was used to measure the protein concentration. Protein was separated in equal quantities using sodium dodecyl sulfate-polyacrylamide gel electrophoresis (SDS-PAGE) at a concentration of 10% (S0690, Beyotime, Shanghai, China). The protein was then transferred onto polyvinylidene fluoride (PVDF) membranes (FFP24, Beyotime, Shanghai, China). Membranes were blocked at room temperature with 5% non-fat milk for one hour. Following blocking, membranes were incubated for one night (4 ℃) with primary antibodies (1:1000) and then (room temperature) with secondary antibodies coupled with horseradish peroxidase (1:2000) for two hours. The ChemiDocTM

Table 1. Sequences of shRNAs used in the experiment.

Name	Sequence (5′-3′)	Carrier name
shNC	CCTAAGGTTAAGTCGCCCTCG	pRP [shRNA]-EGFP-U6>Scramble_shRNA
shGNB2#1	CCTGGATGACAACCAAATCAT	pRP [shRNA]-EGFP-U6>hGNB2 [shRNA#1]
shGNB2#2	CGGCCATGAATCCGACATCAA	pRP [shRNA]-EGFP-U6>hGNB2 [shRNA#2]
shGNB2#3	CGACATCAATGCAGTGGCTTT	pRP [shRNA]-EGFP-U6>hGNB2 [shRNA#3]
NC	CTAGAGAACCCACTGCTTAC	pRP [Exp]-EGFP-CMV
PPARγ		pRP [Exp]-EGFP-CMV>hPPARG [NM_015869]
GNB2		pRP [Exp]-EGFP-CMV>hGNB2 [NM_005273]

shNC, short hairpin RNA negative control; GNB2, G protein subunit beta 2; NC, negative control; PPARγ, peroxisome proliferator-activated receptor gamma.

Table 2. Primers used for real-time PCR in this study.

Genes	Forward primer (5′-3′)	Reverse primer (5′-3′)
GNB2	CAGCAGACAGTGGGTTTTGC	TCATGGCCGATGAAGGTCTG
PPARγ	TTACACAATGCTGGCCTCCTT	AGGCTTTCGCAGGCTCTTTAG
β-actin	TGTTACCAACTGGGACGACA	TCTCAGCTGTGGTGGTGAAG

PCR, polymerase chain reaction.

XRS Imaging System (Bio-Rad, Hercules, CA, USA) and a chemiluminescent (ECL) Western Blotting Detection Kit (KGC4902, Keygene, Nanjing, China) were utilized for discovering protein signals. ImageJ 1.54p (NIH, Bethesda, MD, USA) was applied to quantify the protein band intensity. The antibodies that were employed are listed in Table 3.

Cell Proliferation

After being seeded in 6-well plates, KGN cells were cultivated for 24 hours in DMEM supplemented with 10% FBS. Following the recommended treatments above, the BeyoClickTM 5-ethynyl-2′-deoxyuridine (EdU) Cell Proliferation Detection Kit (C0071S, Beyotime, Shanghai, China) was adopted to quantify cell proliferation according to the manufacturer's instructions. After two hours of incubation with 10 µM EdU labeling solution (37 °C), the cells were fixed for 15 minutes with 4% paraformaldehyde (CF189021, Solarbio, Beijing, China) and permeabilized for 10 minutes with 0.3% Triton X-100 (ST797, Beyotime, Shanghai, China). After 30 minutes of incubation with the EdU kit's Click reaction mixture (room temperature), the cells were shielded from light and stained for 10 minutes with 2-(4-Aminophenyl)-6-indolecarbazole dihydrochloride (DAPI, C1002, Beyotime, Shanghai, China). A Leica DMI3000B inverted fluorescence microscope (200×, Leica, Wetzlar, Germany) served to take fluorescence pictures. ImageJ software served to count the cells. The following formula was adopted to determine the proportion of EdU-positive cells: EdU-positive cells (%) = (green EdU-stained cells / blue DAPI-stained cells) × 100.

Cell Apoptosis

The terminal deoxynucleotidyl transferase dUTP nick end labeling (TUNEL) test was performed to measure apoptosis. Following the manufacturer's instructions, the TUNEL test was carried out using the In Situ Cell Death Detection Kit (C1086, Beyotime, Shanghai, China). KGN cells were treated as directed after being seeded on coverslips in 6-well plates (BS-CP-6C, Biosharp, Hefei, China). Following the procedure, cells were fixed for 15 minutes using 4% paraformaldehyde (room temperature). After that, cells were permeabilized for ten minutes using 0.3% Triton X-100. Cells were washed with phosphate-buffered saline (PBS, C0221A, Shanghai, China) and then treated with 50 µL of TUNEL reaction mixture at 37 °C for one hour. After that, the samples were dyed using DAPI at room temperature for ten minutes. Fluorescence images were captured using a 200× fluorescence microscope. Cell counting was performed using ImageJ software. TUNEL-positive staining was visualized in green, whereas DAPI-positive nuclei were visualized in blue.

Pyruvate and Lactate Levels

KGN cells were homogenized, and the supernatants were collected by centrifugation. The concentrations of pyruvate and lactate in the culture media were determined using Pyruvate Assay Kits (A081-1-1, Nanjing Jiancheng Bioengineering Institute, Nanjing, China) and Lactate Assay Kits (A019-2-1, Nanjing Jiancheng Bioengineering Institute, Nanjing, China), respectively. A microplate reader (Bio-Rad, Hercules, CA, USA) was applied to identify absorbance at 530 nm.

Table 3. Antibodies used in Western blot analysis.

Antibody name	Molecular weight	Source	Catalog number	Supplier	Type
PPARγ	58 kDa	Rabbit	ab178860	Abcam	Primary antibody
PKM2	57 kDa	Rabbit	ab150377	Abcam	Primary antibody
GNB2	35 kDa	Rabbit	ab108504	Abcam	Primary antibody
β-actin	42 kDa	Rabbit	ab8227	Abcam	Primary antibody
Goat Anti-Rabbit IgG H&L (HRP)	N/A	Goat	ab6721	Abcam	Secondary antibody

PKM2, pyruvate kinase m2.

Binding Site Prediction

Potential binding sites within the GNB2 promoter were predicted using the University of California, Santa Cruz Genome (UCSC) database (http://genome.ucsc.edu/) and the Joint Conservation of Transcription Factor Binding Profiles Across Species (JASPAR) database (https://jaspar.genereg.net/).

Chromatin Immunoprecipitation (ChIP) Assay

ChIP experiments were performed using the Chromatin Immunoprecipitation Kit (P2078, Beyotime, Shanghai, China) in line with the manufacturer's instructions to confirm that PPARγ bound to the GNB2 promoter. To summarize, KGN cells were collected, sonicated, and then thrice washed with 1 mL PBS containing phenylmethylsulfonyl fluoride (PMSF, ST507, Beyotime, Shanghai, China). 1% formaldehyde (C06701102, Nanjing Reagents, China) was administered to crosslink cells at room temperature for 15 minutes. Then, Glycine solution (ST085, Beyotime, Shanghai, China) was added to quench the crosslinking, and it was incubated at room temperature for five minutes. The pellets were centrifuged and then washed thrice with PBS containing PMSF. After resuspending the pellets in SDS lysis solution (SL1031, Coolaber, Beijing, China) containing PMSF, they were sonicated for five minutes after being incubated on ice for ten minutes. Following that, 1.8 mL of ChIP dilution buffer containing 1 mM PMSF was administered to dilute the samples. The sample was stored in 20 microliters to be used as the input for further detection. To lessen the non-specific binding of Protein A + G Agarose/Salmon Sperm DNA to target proteins or DNA sequences, the remaining samples were gently rotated while incubated with 70 µL of the mixture at 4 ℃ for 30 minutes. The supernatant was transferred to a 2 mL centrifuge tube (F601621, Shenggong Bio, Shanghai, China) following centrifugation for one minute (1000 ×g, 4 ℃). After adding anti-PPARγ (1:200, ab310323, Abcam, Cambridge, UK) or negative control IgG (1:200, ab313801, Abcam, Cambridge, UK) antibodies, the mixture was gently rotated and incubated at 4 ℃ for the whole night. The pellets were resuspended in 25 µL SDS-PAGE protein sample solution (P0015A, Beyotime, Shanghai, China) after washing with low-salt immune complex wash buffer, high-salt immune complex wash buffer, LiCl immune complex wash buffer, and Tris-Ethylenediaminetetraacetic acid buffer. DNA fragments were recovered by eluting protein-DNA complexes with elution buffer (C600325-0500, Shenggong Bio, Shanghai, China). As described above, RT-qPCR was used to identify the enrichment of PPARγ at the GNB2 promoter region.

Dual-Luciferase Reporter Assay

To create luciferase reporter gene vectors, wild-type PPARγ (WT-PPARγ) and mutant PPARγ (MUT-PPARγ) were cloned into the pGL3-Basic plasmid (HG-VQP0121, Promega, Madison, WI, USA). The NC was the empty pGL3-Basic plasmid (WT/MUT-empty vector), and the pRL-SV40 Renilla luciferase reporter gene plasmid (P2149, Shanghai Huzhen Industrial Co., Ltd., Shanghai, China) served as an internal control. KGN cells were co-transfected with the recombinant plasmids and incubated for 36 hours. After that, 100 µL of passive lysis buffer (YB25-191208, Shanghai Yubo Biotech, Shanghai, China) was administered to lyse the cells. Luciferase activity in the cell lysates was measured using the Dual-Luciferase Reporter Assay System (E1910, Promega, Madison, WI, USA). The level of activity of each luciferase was compared.

Immunoprecipitation (IP)

Five experimental groups were established from KGN cells: immunoglobulin G (IgG), GNB2-antibody (GNB2-Ab), GNB2-Ab+GNB2, GNB2-Ab+MG132, and GNB2-Ab+MG132+GNB2. Two micrograms per milliliter of IgG (1:20, ab172730, Abcam, Cambridge, UK) and GNB2-Ab (1:1000; ab108504, Abcam, Cambridge, UK) were administered to KGN cells in the IgG and GNB2-Ab groups for one hour. For the GNB2-Ab+GNB2, GNB2-Ab+MG132, and GNB2-Ab+MG132+GNB2 groups, KGN cells were transfected with the GNB2 overexpression vector for 48 hours, followed by treatment with 10 µM MG-132 for 6 hours, and then treated with GNB2-Ab. IP was performed using Protein A/G PLUS-Agarose (sc-2003, Santa Cruz Biotechnology, Inc., Dallas, TX, USA). In particular, cell lysates were obtained by sonicating KGN cells in RIPA buffer. GNB2 and PKM2 levels were measured by WB analysis of total protein levels. For IP, a primary antibody against PKM2 (1:200, ab137791, Abcam, Cambridge, UK) was incubated with 20 µg of total protein at 4 ℃ for two hours. Centrifugation was applied to collect the precipita-

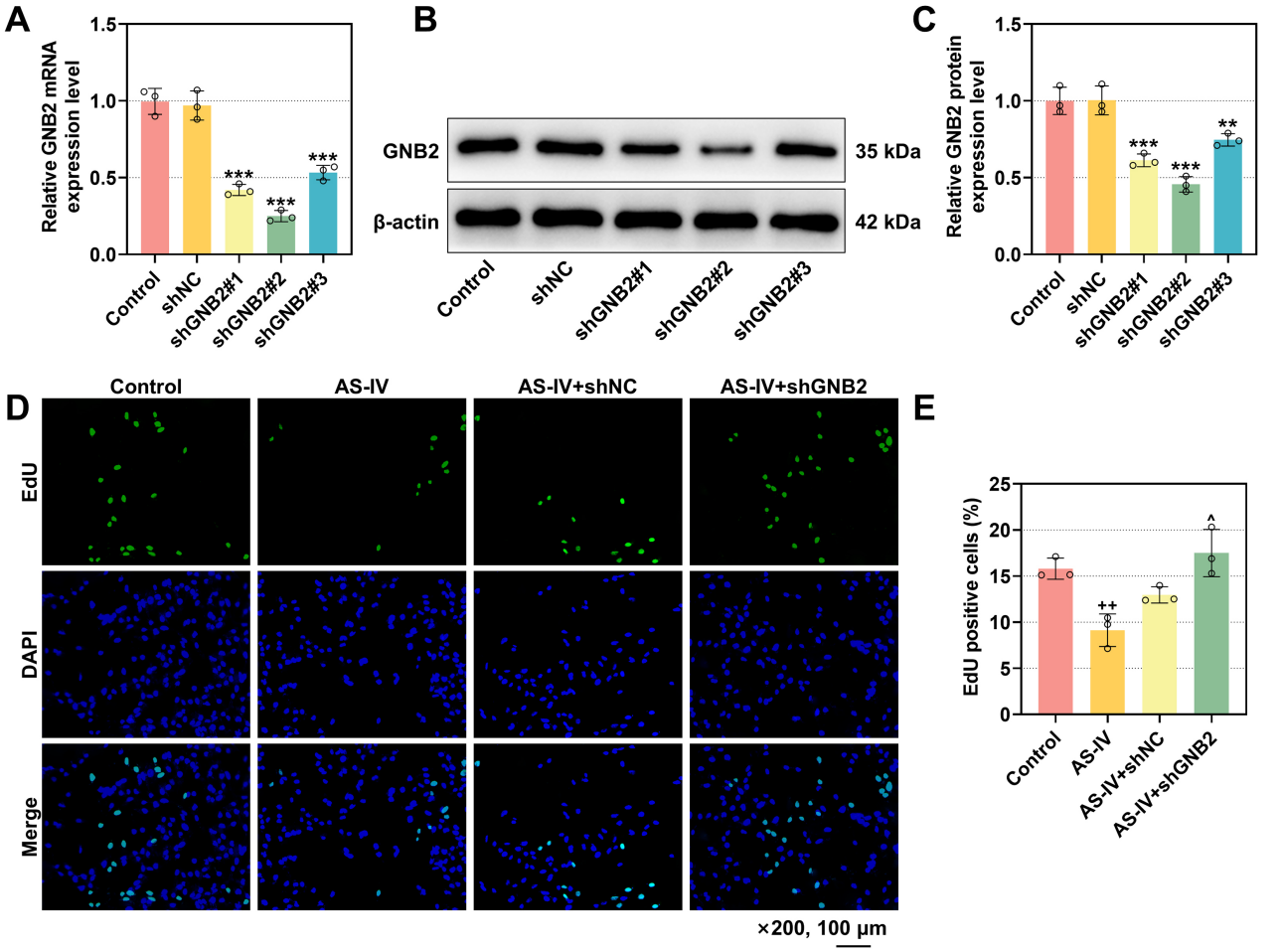

Fig. 1. G protein subunit beta 2 (GNB2) gene knockdown and astragaloside IV (AS-IV) treatment in human ovarian granulosa cell tumor (KGN) cells and their effect on proliferation. (A) Reverse transcription quantitative polymerase chain reaction (RT-qPCR) analysis of *GNB2* mRNA levels in KGN cells from Control, short hairpin RNA negative control (shNC), shRNA targeting GNB2 (shGNB2)#1, shGNB2#2, and shGNB2#3 groups, with *β-actin* as the reference. (B,C) Western blot analysis of GNB2 protein levels in KGN cells from Control, shNC, shGNB2#1, shGNB2#2, and shGNB2#3 groups, with β-actin as the reference. (D) 5-ethynyl-2′-deoxyuridine (EdU) assay to detect KGN cell proliferation in Control, AS-IV, AS-IV+shNC, and AS-IV+shGNB2 groups. Magnification: 200×, scale bar: 100 μm. EdU-positive cells are green, and nuclei are blue. (E) Quantitative analysis of the EdU assay. Each experiment was repeated independently three times. $^{**}p < 0.01$,$^{***}p < 0.001$ vs. shNC; $^{++}p < 0.01$ vs. Control; $^{\wedge}p < 0.05$ vs. AS-IV+shNC.

tion after adding Protein A/G agarose beads and incubating for an additional hour. The precipitate was thoroughly cleaned and then resuspended in 20 μL of SDS sample buffer (P0015L, Beyotime, Shanghai, China). SDS-PAGE served to resolve protein complexes, which were then transferred onto PVDF membranes. After blocking the membranes with 5% non-fat milk, they were incubated with the primary antibody Anti-Ubiquitin (1:1000, ab140601, Abcam, Cambridge, UK) at 4 °C for whole night. Following incubation with the secondary antibody (1:5000, ab205718, Abcam, Cambridge, UK), protein signals were identified using the ChemiDocTM XRS Imaging System and an ECL reagent.

To validate the interaction between GNB2 and the ubiquitin ligases NEDD4-like E3 ubiquitin protein ligase (NEDD4L)/NEDD4 E3 ubiquitin protein ligase (NEDD4), co-immunoprecipitation (Co-IP) was performed. Briefly, KGN cell lysates were incubated overnight at 4 °C with an antibody against GNB2 (1:20, RAB01735, Thermo Fisher Scientific, Waltham, MA, USA). Normal rabbit IgG was used as a negative control. Protein A/G Sepharose beads were then added to capture the immune complexes. After washing, bound proteins were eluted in SDS-PAGE loading buffer. The eluates were then analyzed by Western blotting with specific antibodies to detect whether NEDD4 (2–10 μg/mg, ab117826, Abcam, Cambridge, UK) and NEDD4L (1:50, #4013, CST, Danvers, MA, USA) were co-precipitated with GNB2. Input lysates (representing 5% of the starting material) served as a loading control to verify the presence of all proteins of interest.

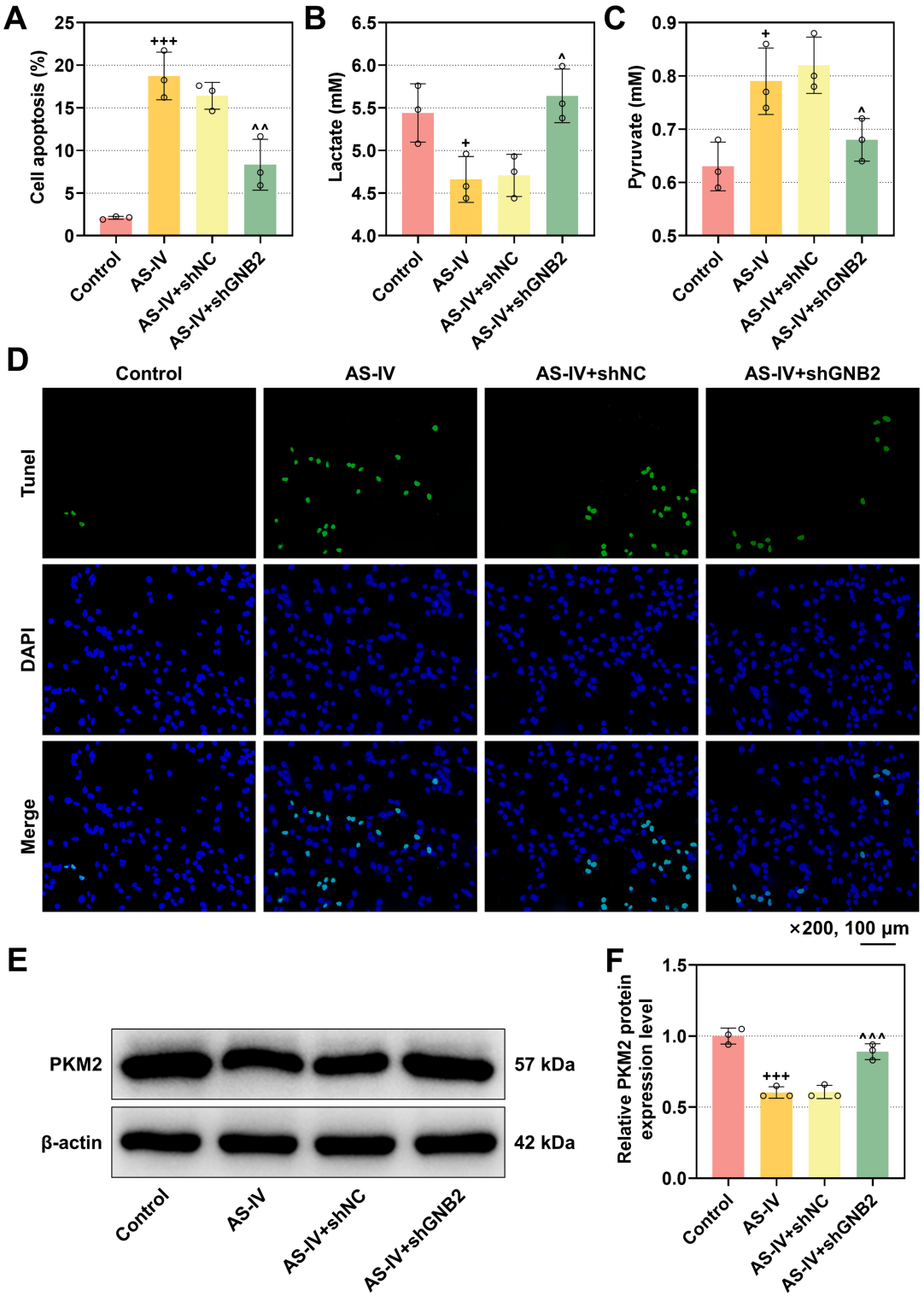

Fig. 2. AS-IV effects on cell apoptosis, lactate, pyruvate, and pyruvate kinase m2 (PKM2) expression. (A,D) Terminal deoxynucleotidyl transferase dUTP nick end labeling (TUNEL) staining to detect apoptosis in KGN cells from Control, AS-IV, AS-IV+shNC, and AS-IV+shGNB2 groups. Magnification: 200×, scale bar: 100 μm. TUNEL-positive cells are green, and nuclei are blue. (B,C) Kit-based measurement of lactate and pyruvate levels in KGN cells from Control, AS-IV, AS-IV+shNC, and AS-IV+shGNB2 groups. (E,F) Western blot analysis of PKM2 protein expression in KGN cells from Control, AS-IV, AS-IV+shNC, and AS-IV+shGNB2 groups, with β-actin as the reference. Each experiment was repeated independently three times. $^{+}p < 0.05$, $^{+++}p < 0.001$ vs. Control; $^{\wedge}p < 0.05$, $^{\wedge\wedge}p < 0.01$, $^{\wedge\wedge\wedge}p < 0.001$ vs. AS-IV+shNC.

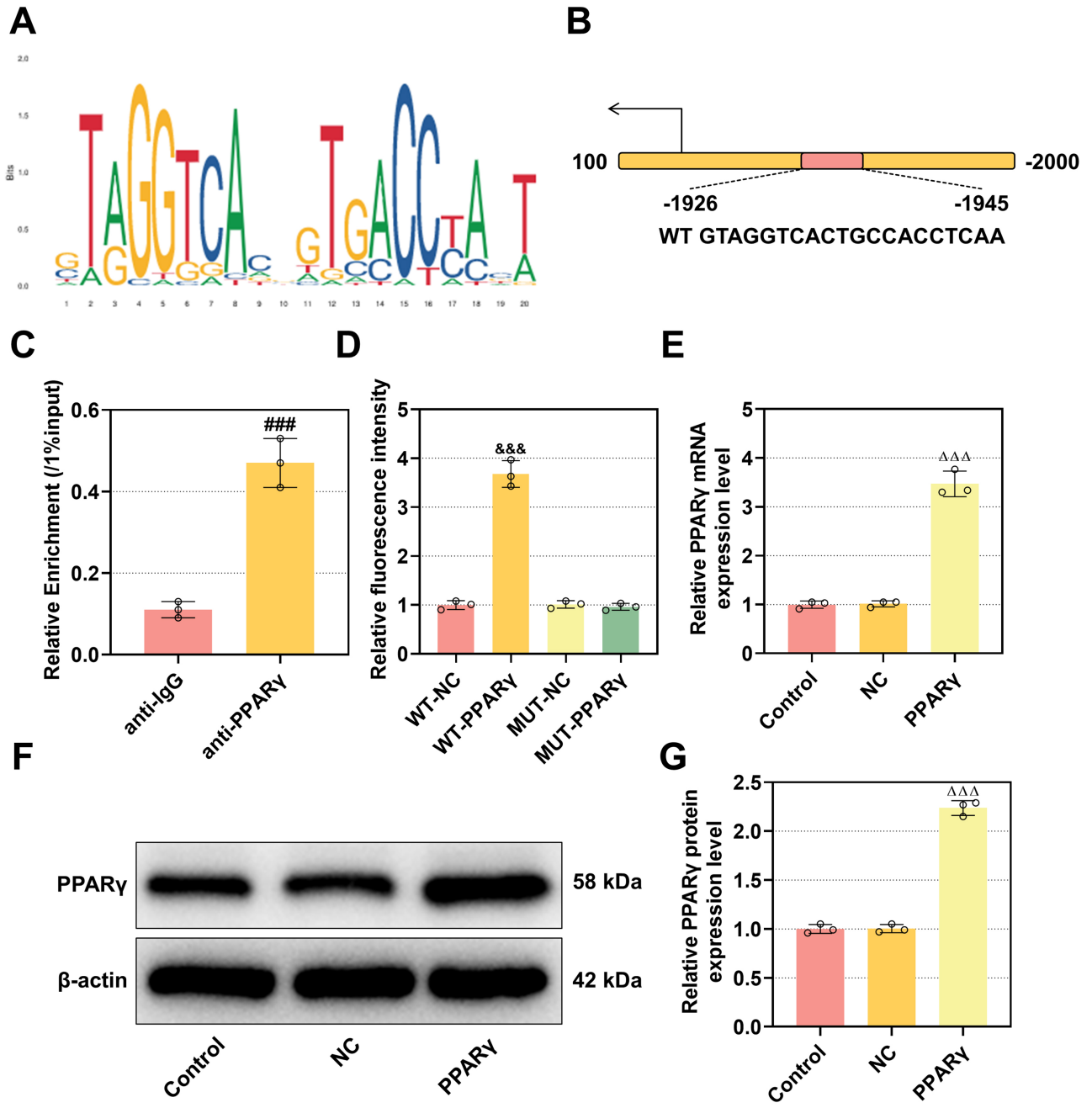

Fig. 3. Peroxisome proliferator activated receptor gamma (PPARγ) binding to the GNB2 promoter and its regulation. (A,B) Joint Conservation of Transcription Factor Binding Profiles Across Species (JASPAR) database prediction of the binding sites between PPARγ and the GNB2 promoter region. (C) Chromatin immunoprecipitation (ChIP) analysis of the binding of PPARγ to GNB2. (D) Dual-luciferase reporter assay to detect the binding sites of PPARγ on the GNB2 promoter. (E) RT-qPCR analysis of *PPARγ* mRNA levels in KGN cells from Control, NC, and PPARγ groups, with *β-actin* as the reference. (F,G) Western blot analysis of PPARγ protein levels in KGN cells from Control, NC, and PPARγ groups, with β-actin as the reference. Each experiment was repeated independently three times. $^{###}p < 0.001$ vs. anti-IgG; $^{\&\&\&}p < 0.001$ vs. WT-NC; $^{\Delta\Delta\Delta}p < 0.001$ vs. NC.

Statistical Analysis

Software called GraphPad 8.0 (GraphPad Software, San Diego, CA, USA) was implemented to conduct statistical analyses. One-way ANOVA followed by Tukey's post-hoc test was adopted for comparisons between multiple groups, while the independent samples *t*-test was performed for comparisons between two groups. A $p < 0.05$ is considered as a statistically significant difference.

Results

AS-IV Regulates the Proliferation, Apoptosis, and Glycolysis of KGN Cells by Activating GNB2

We transfected KGN cells with shGNB2 to suppress its expression to examine the function of GNB2 in KGN cells. Transfection with shGNB2#1, shGNB2#2, and shGNB2#3 drastically lowered GNB2 levels, according to RT-qPCR and WB analyses ($p < 0.01$, Fig. 1A–C). The most significant impact was observed in shGNB2#2, which was employed in further studies ($p < 0.001$, Fig. 1A–C). KGN cell proliferation was diminished by AS-IV treatment, and the effects of AS-IV were partially restored by GNB2 knockdown ($p < 0.05$, Fig. 1D,E). The AS-IV group showed lower levels of lactate and PKM2, as well as higher levels of pyruvate and cell apoptosis (green fluorescence) compared to the Control group ($p < 0.05$, Fig. 2A–F). Conversely, the AS-IV+shGNB2 group displayed higher levels of lactate and PKM2 and lower levels of pyruvate and apoptosis (green fluorescence) in the AS-IV+shNC group ($p < 0.05$, Fig. 2A–F).

AS-IV Promotes KGN Cell Apoptosis by Transcriptionally Regulating GNB2 Through PPARγ

JASPAR analysis showed that PPARγ was enriched in the GNB2 promoter region, and one potential binding site, GTAGGTCACTGCCACCTCAA, was selected for further validation (Fig. 3A,B). Additionally, ChIP experiments demonstrated that PPARγ is concentrated in the GNB2 promoter ($p < 0.001$, Fig. 3C). Dual-luciferase reporter tests showed that WT-PPARγ had a much greater relative luciferase activity than WT-NC ($p < 0.001$, Fig. 3D), whereas the MUT group showed no discernible change (Fig. 3D). PPARγ overexpression markedly increased PPARγ levels in KGN cells, according to RT-qPCR and WB analyses ($p < 0.001$, Fig. 3E–G). Overexpression of PPARγ enhanced the inhibitory effect of AS-IV on the proliferation of KGN cells and promoted cell death, while GNB2 knockdown partially reversed the effects of PPARγ overexpression ($p < 0.05$, Fig. 4A–D).

AS-IV Inhibits KGN Cell Glycolysis by Promoting the Ubiquitination and Degradation of PKM2 Through the PPARγ/GNB2

The AS-IV+PPARγ group showed higher pyruvate levels and lower lactate and PKM2 levels over the AS-IV+NC group ($p < 0.05$, Fig. 5A–D). As opposed to the AS-IV+PPARγ+shNC group, the AS-IV+PPARγ+shGNB2 group displayed lower pyruvate levels and higher lactate and PKM2 levels ($p < 0.05$, Fig. 5A–D). In KGN cells, GNB2 overexpression increased its own levels and decreased PKM2 expression. MG132 treatment partially restored PKM2 levels, supporting that GNB2 promotes PKM2 degradation via the proteasome ($p < 0.05$, Fig. 5E–G). Ubiquitination assays confirmed that GNB2 overexpression enhanced poly-ubiquitination of PKM2, which accumulated further upon MG132 treatment (Fig. 5H). We next sought to identify the mechanistic link between GNB2 and PKM2 ubiquitination. Coimmunoprecipitation assays revealed that GNB2 specifically interacts with the E3 ubiquitin ligases NEDD4L and NEDD4 in KGN cells (Fig. 5I,J). Together, these results indicate that GNB2 likely facilitates PKM2 degradation by directly recruiting NEDD4L/NEDD4, thereby promoting PKM2 ubiquitination and proteasomal degradation.

Discussion

Research has indicated that GC proliferation is higher in people with PCOS, and this aberrant proliferation is intimately associated with ovarian dysfunction and the pathophysiology of PCOS [22]. In this study, we found that AS-IV treatment inhibited the proliferation of KGN cells and promoted apoptosis. Notably, further investigation revealed that the knockdown of GNB2 could reverse AS-IV-induced inhibition of proliferation and promotion of apoptosis, suggesting that GNB2 plays a crucial role in the cell regulation process mediated by AS-IV. GNB2, a G protein beta subunit, plays a crucial role in cellular signal transduction [23]. In addition to controlling G protein-coupled receptor (GPCR) signaling pathways, it serves a role in apoptosis, metabolic regulation, and cell division [24]. Our results show that AS-IV primarily regulates KGN cell proliferation and apoptosis through GNB2.

PPARγ, a nuclear receptor transcription factor, is vital in regulating inflammation, cell differentiation, and lipid metabolism [25]. Abnormal activation of PPARγ has been closely linked to various metabolic diseases. In adipose tissue, PPARγ regulates insulin sensitivity, and its abnormal activation leads to defective adipocyte differentiation, excessive fat accumulation, and insulin resistance, promoting the development of type 2 diabetes mellitus (T2DM) [26,27]. In the liver, aberrant activation of PPARγ can drive hepatic fat accumulation, worsen hepatocyte steatosis, and contribute to the progression of non-alcoholic fatty liver disease to non-alcoholic steatohepatitis and even liver fibrosis [28,29]. In this study, we found that PPARγ transcriptionally regulates GNB2 expression, which in turn inhibits the proliferation of KGN cells. These results suggest that AS-IV may upregulate GNB2 expression by activating the PPARγ, thereby regulating glycolytic metabolism and inhibiting the abnormal proliferation of KGN cells.

Glycolysis is a metabolic pathway in which glucose is converted to pyruvate, producing energy and playing a key role in cellular energy supply, particularly under anaerobic conditions [30]. Glycolysis is crucial not only in normal physiological processes but also in the development of various diseases. Ovarian GC in PCOS patients exhibits elevated glycolysis levels, leading to energy metabolism disorders that affect follicular development [31]. Insulin resistance in PCOS patients is associated with abnormal glycolysis, and an overactive glycolysis pathway may im-

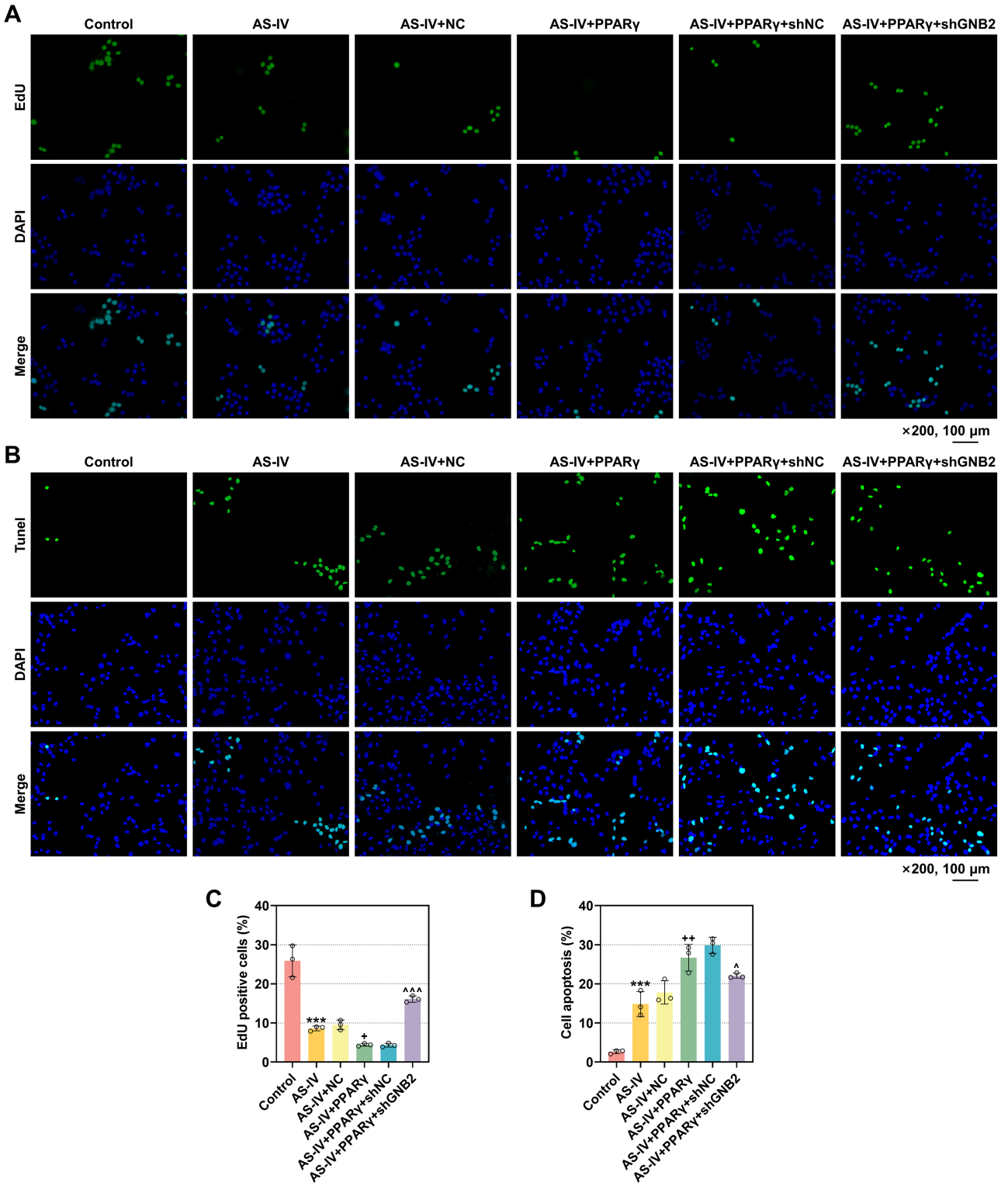

Fig. 4. Effect of PPARγ on cell proliferation and apoptosis. (A,C) 5-ethynyl-2′-deoxyuridine (EdU) assay to detect KGN cell proliferation in Control, AS-IV, AS-IV+NC, AS-IV+PPARγ, AS-IV+PPARγ+shNC, and AS-IV+PPARγ+shGNB2 groups. Magnification: 200×, scale bar: 100 μm. EdU-positive cells are green, and nuclei are blue. (B,D) TUNEL staining to detect KGN cell apoptosis in the Control, AS-IV, AS-IV+NC, AS-IV+PPARγ, AS-IV+PPARγ+shNC, and AS-IV+PPARγ+shGNB2 groups. Magnification: 200×, scale bar: 100 μm. TUNEL-positive cells are green, and nuclei are blue. Each experiment was repeated independently three times. $^{***}p < 0.001$ vs. Control; $^{+}p < 0.05$, $^{++}p < 0.01$ vs. AS-IV+NC; $^{\wedge}p < 0.05$, $^{\wedge\wedge\wedge}p < 0.001$ vs. AS-IV+PPARγ+shNC.

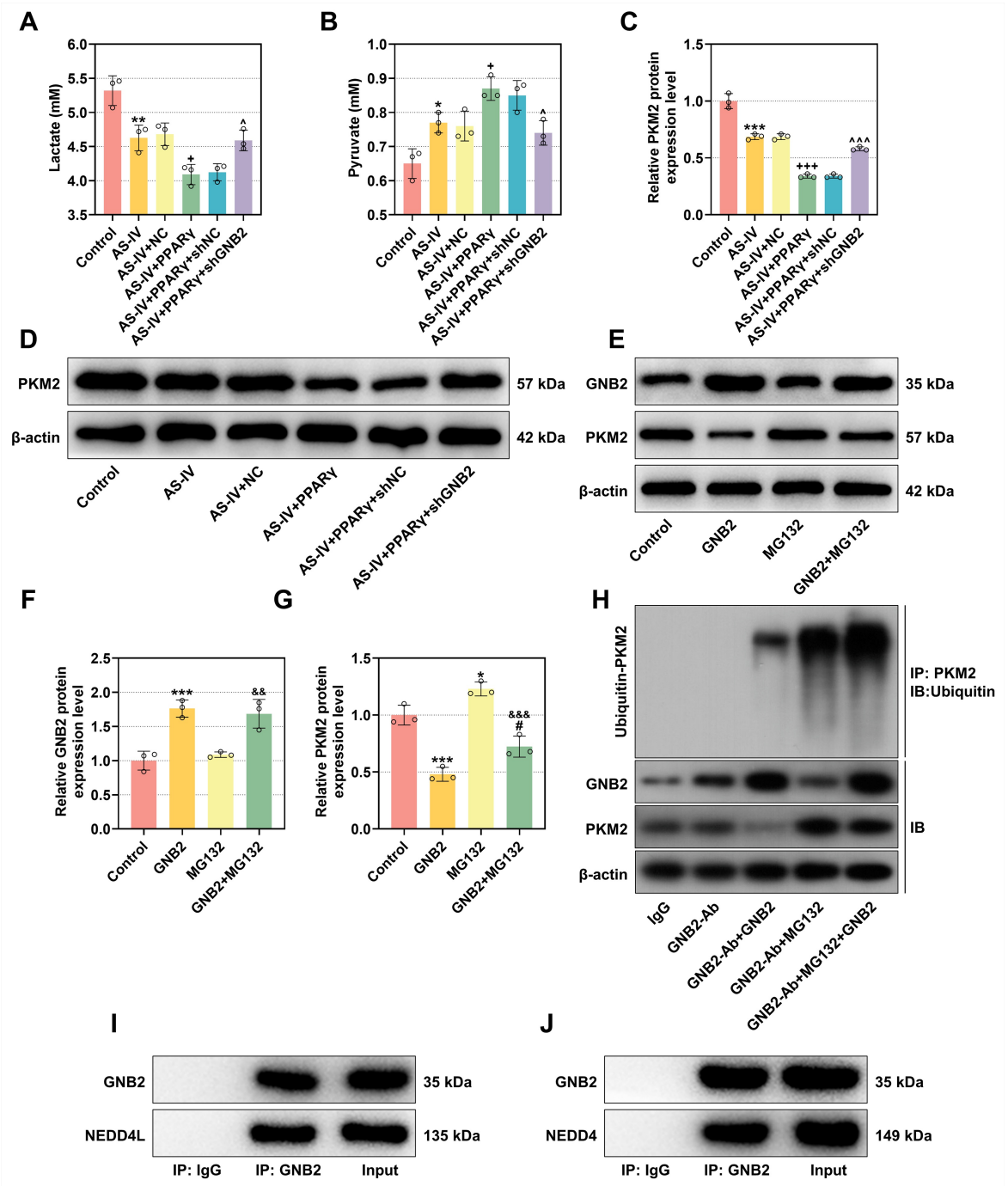

Fig. 5. AS-IV regulates glycolysis and PKM2 degradation via GNB2. (A,B) Kit-based measurement of lactate and pyruvate levels in KGN cells from Control, AS-IV, AS-IV+NC, AS-IV+PPARγ, AS-IV+PPARγ+shNC, and AS-IV+PPARγ+shGNB2 groups. (C,D) Western blot analysis of PKM2 protein levels in KGN cells from Control, AS-IV, AS-IV+NC, AS-IV+PPARγ, AS-IV+PPARγ+shNC, and AS-IV+PPARγ+shGNB2 groups, with β-actin as the reference. (E–G) Western blot analysis of GNB2 and PKM2 protein levels in KGN cells from Control, GNB2, Z-Leu-Leu-Leu-al (MG132), and GNB2+MG132 groups, with β-actin as the reference. (H) Immunoprecipitation and Western blot analysis to detect PKM2 ubiquitination levels in KGN cells from immunoglobulin G (IgG), GNB2-antibody (GNB2-Ab), GNB2-Ab+GNB2, GNB2-Ab+MG132, and GNB2-Ab+MG132+GNB2 groups, with β-actin as the reference. (I) Co-IP detection of GNB2 interacting with NEDD4-like E3 ubiquitin protein ligase (NEDD4L) in KGN cells. (J) Co-IP detection of GNB2 interacting with NEDD4 E3 ubiquitin protein ligase (NEDD4) in KGN cells. Each experiment was repeated independently three times. $^{*}p < 0.05$, $^{**}p < 0.01$, $^{***}p < 0.001$ vs. Control; $^{+}p < 0.05$, $^{+++}p < 0.001$ vs. AS-IV+NC; $^{\wedge}p < 0.05$, $^{\wedge\wedge\wedge}p < 0.001$ vs. AS-IV+PPARγ+shNC; $^{\#}p < 0.05$ VS. GNB2; $^{\&\&}p < 0.01$, $^{\&\&\&}p < 0.001$ vs. MG132.

pair insulin signaling and exacerbate metabolic disorders [32]. PKM2 is a rate-limiting enzyme in the glycolysis process and plays a crucial role in regulating cellular energy metabolism and growth. Previous study has reported that PKM2 degradation through ubiquitination is regulated by various E3 ubiquitin ligases, including NEDD4L, NEDD4, and GNB2 [18]. The ubiquitin-proteasome system (UPS) regulates the stability, degradation, and function of proteins by ubiquitination, a significant post-translational modification that is extensively implicated in metabolic regulation, cellular signal transmission, and the advancement of illness [33]. In this study, we found that GNB2 promotes the ubiquitination and proteasomal degradation of PKM2. Lactic acid and pyruvate are the major metabolic products of glycolysis, with lactic acid serving as the end product of anaerobic glycolysis, which can accumulate in tumor cells and other high metabolic states [34]. Pyruvate is a key intermediate in glycolysis and can further enter the mitochondria to participate in the tricarboxylic acid (TCA) cycle, thereby influencing cellular energy metabolism [35]. In this study, we found that AS-IV, by upregulating the PPARγ/GNB2, inhibits PKM2 expression, decreases lactate levels, and increases pyruvate content, thereby influencing the glycolytic metabolism. These findings suggest that AS-IV may regulate glycolysis to suppress the abnormal proliferation of granulosa cells. While this study focused on the role of GNB2 and PPARγ within the AS-IV-activated pathway, elucidating its intrinsic functions under basal conditions represents an important direction for future research.

This study has several limitations. First, the experiments were primarily conducted using the KGN cell line, which, although providing valuable mechanistic insights, cannot fully reflect the complex physiological environment *in vivo*. Further validation using animal models is warranted. Second, although the AS-IV dosage *in vitro* was optimized, its therapeutic dose range, efficacy, and safety in clinical settings require further investigation.

Conclusion

In conclusion, this study demonstrates that AS-IV regulates glycolysis through the PPARγ/GNB2/PKM2 axis, thereby modulating the proliferation and apoptosis of KGN cells. AS-IV inhibits cell proliferation and promotes apoptosis by activating GNB2, and the knockdown of GNB2 partially reverses these effects. Mechanistically, PPARγ transcriptionally upregulates GNB2 expression, enhancing the inhibitory effect of AS-IV on proliferation. Furthermore, GNB2 facilitates the ubiquitination and proteasomal degradation of PKM2, thereby regulating glycolytic activity. These results highlight the significant role of the PPARγ/GNB2/PKM2 pathway in regulating KGN cell metabolism and proliferation.

Availability of Data and Materials

The analyzed data sets generated during the study are available from the corresponding author on reasonable request.

Author Contributions

WCZ, MXW and SZZ designed the research study; BW performed the research; JJ collected and analyzed the data. MXW has been involved in drafting the manuscript and all authors have been involved in revising it critically for important intellectual content. All authors gave final approval of the version to be published. All authors have participated sufficiently in the work to take public responsibility for appropriate portions of the content and agreed to be accountable for all aspects of the work in ensuring that questions related to its accuracy are addressed.

Ethics Approval and Consent to Participate

Not applicable.

Acknowledgment

Not applicable.

Funding

This work was supported by Zhejiang Province Traditional Chinese Medicine Science and Technology Project under Grant [number 2024ZR078].

Conflict of Interest

The authors declare no conflict of interest.

Supplementary Material

Supplementary material associated with this article can be found, in the online version, at https://doi.org/10.24976/Discov.Med.202638208.125.

References

[1] Siddiqui S, Mateen S, Ahmad R, Moin S. A brief insight into the etiology, genetics, and immunology of polycystic ovarian syndrome (PCOS). Journal of Assisted Reproduction and Genetics. 2022; 39: 2439–2473. https://doi.org/10.1007/s10815-022-02625-7.

[2] Armanini D, Boscaro M, Bordin L, Sabbadin C. Controversies in the Pathogenesis, Diagnosis and Treatment of PCOS: Focus on Insulin Resistance, Inflammation, and Hyperandrogenism. International Journal of Molecular Sciences. 2022; 23: 4110. https://doi.org/10.3390/ijms23084110.

[3] Meier RK. Polycystic Ovary Syndrome. The Nursing Clinics of North America. 2018; 53: 407–420. https://doi.org/10.1016/j.cnur.2018.04.008.

[4] Nisa KU, Tarfeen N, Mir SA, Waza AA, Ahmad MB, Ganai BA. Molecular Mechanisms in the Etiology of Polycystic Ovary Syndrome (PCOS): A Multifaceted Hypothesis Towards the Disease with Potential Therapeutics. Indian Journal of Clinical Biochemistry: IJCB. 2024; 39: 18–36. https://doi.org/10.1007/s12291-023-01130-7.

[5] Arvanitakis K, Chatzikalil E, Kalopitas G, Patoulias D, Popovic DS, Metallidis S, *et al*. Metabolic Dysfunction-Associated Steatotic Liver Disease and Polycystic Ovary Syndrome: A Complex Interplay. Journal of Clinical Medicine. 2024; 13: 4243. https://doi.org/10.3390/jcm13144243.

[6] Zeng LH, Rana S, Hussain L, Asif M, Mehmood MH, Imran I, *et al*. Polycystic Ovary Syndrome: A Disorder of Reproductive Age, Its Pathogenesis, and a Discussion on the Emerging Role of Herbal Remedies. Frontiers in Pharmacology. 2022; 13: 874914. https://doi.org/10.3389/fphar.2022.874914.

[7] Gu Y, Zhou G, Zhou F, Wu Q, Ma C, Zhang Y, *et al*. Life Modifications and PCOS: Old Story But New Tales. Frontiers in Endocrinology. 2022; 13: 808898. https://doi.org/10.3389/fendo.2022.808898.

[8] Rashid R, Mir SA, Kareem O, Ali T, Ara R, Malik A, *et al*. Polycystic ovarian syndrome-current pharmacotherapy and clinical implications. Taiwanese Journal of Obstetrics & Gynecology. 2022; 61: 40–50. https://doi.org/10.1016/j.tjog.2021.11.009.

[9] Singh S, Pal N, Shubham S, Sarma DK, Verma V, Marotta F, *et al*. Polycystic Ovary Syndrome: Etiology, Current Management, and Future Therapeutics. Journal of Clinical Medicine. 2023; 12: 1454. https://doi.org/10.3390/jcm12041454.

[10] Li L, Zhang Y, Luo Y, Meng X, Pan G, Zhang H, *et al*. The Molecular Basis of the Anti-Inflammatory Property of Astragaloside IV for the Treatment of Diabetes and Its Complications. Drug Design, Development and Therapy. 2023; 17: 771–790. https://doi.org/10.2147/DDDT.S399423.

[11] Yang C, Pan Q, Ji K, Tian Z, Zhou H, Li S, *et al*. Review on the protective mechanism of astragaloside IV against cardiovascular diseases. Frontiers in Pharmacology. 2023; 14: 1187910. https://doi.org/10.3389/fphar.2023.1187910.

[12] Gao Y, Su X, Xue T, Zhang N. The beneficial effects of astragaloside IV on ameliorating diabetic kidney disease. Biomedicine & Pharmacotherapy = Biomedecine & Pharmacotherapie. 2023; 163: 114598. https://doi.org/10.1016/j.biopha.2023.114598.

[13] Jozkowiak M, Piotrowska-Kempisty H, Kobylarek D, Gorska N, Mozdziak P, Kempisty B, *et al*. Endocrine Disrupting Chemicals in Polycystic Ovary Syndrome: The Relevant Role of the Theca and Granulosa Cells in the Pathogenesis of the Ovarian Dysfunction. Cells. 2022; 12: 174. https://doi.org/10.3390/cells12010174.

[14] Cao LY, Zhang ZQ, Liu PP, Xu DF, Tang L, Fan L, *et al*. Aberrant BMP15/HIF-1α/SCF signaling pathway in human granulosa cells is involved in the PCOS related abnormal follicular development. Gynecological Endocrinology: the Official Journal of the International Society of Gynecological Endocrinology. 2022; 38: 971–977. https://doi.org/10.1080/09513590.2022.2125951.

[15] Wen M, Chen W, Zhou Q, Dou X. Astragaloside IV regulates autophagy-mediated proliferation and apoptosis in a rat model of PCOS by activating the PPARγ pathway. Iranian Journal of Basic Medical Sciences. 2022; 25: 882–889. https://doi.org/10.22038/IJBMS.2022.64475.14179.

[16] Luo J, Zhang L, Guo L, Yang S. PKM2 regulates proliferation and apoptosis through the Hippo pathway in oral tongue squamous cell carcinoma. Oncology Letters. 2021; 21: 461. https://doi.org/10.3892/ol.2021.12722.

[17] Liu T, Zhu S, Sun J, Ma Y. Interactions of tumor necrosis factor receptor-associated factor 4 and pyruvate kinase muscle isoform 2 promote malignant behavior and aerobic glycolysis in colorectal cancer cells. Cytojournal. 2025; 22: 24. https://doi.org/10.25259/Cytojournal_167_2024.

[18] Ding H, Wang JJ, Zhang XY, Yin L, Feng T. Lycium barbarum Polysaccharide Antagonizes LPS-Induced Inflammation by Altering the Glycolysis and Differentiation of Macrophages by Triggering the Degradation of PKM2. Biological & Pharmaceutical Bulletin. 2021; 44: 379–388. https://doi.org/10.1248/bpb.b20-00752.

[19] Xu X, Song X, Xu X, Zheng Y, Xu L, Shen L. Inhibition of sestrin 1 alleviates polycystic ovary syndrome by decreasing autophagy. Aging. 2021; 13: 11774–11785. https://doi.org/10.18632/aging.202872.

[20] Xu F, Cui WQ, Wei Y, Cui J, Qiu J, Hu LL, *et al*. Astragaloside IV inhibits lung cancer progression and metastasis by modulating macrophage polarization through AMPK signaling. Journal of Experimental & Clinical Cancer Research: CR. 2018; 37: 207. https://doi.org/10.1186/s13046-018-0878-0.

[21] Ng HF, Ngeow YF. A simple spreadsheet-based method for relative quantification using quantitative real-time PCR. Biochemistry and Molecular Biology Education: a Bimonthly Publication of the International Union of Biochemistry and Molecular Biology. 2022; 50: 99–103. https://doi.org/10.1002/bmb.21596.

[22] Sun P, Zhang Y, Sun L, Sun N, Wang J, Ma H. Kisspeptin regulates the proliferation and apoptosis of ovary granulosa cells in polycystic ovary syndrome by modulating the PI3K/AKT/ERK signalling pathway. BMC Women's Health. 2023; 23: 15. https://doi.org/10.1186/s12905-022-02154-6.

[23] Tan NB, Pagnamenta AT, Ferla MP, Gadian J, Chung BH, Chan MC, *et al*. Recurrent *de novo* missense variants in *GNB2* can cause syndromic intellectual disability. Journal of Medical Genetics. 2022; 59: 511–516. https://doi.org/10.1136/jmedgenet-2020-107462.

[24] Tan Y, Wang Q, Zhao B, She Y, Bi X. GNB2 is a mediator of lidocaine-induced apoptosis in rat pheochromocytoma PC12 cells. Neurotoxicology. 2016; 54: 53–64. https://doi.org/10.1016/j.neuro.2016.03.015.

[25] Sobolev VV, Tchepourina E, Korsunskaya IM, Geppe NA, Chebysheva SN, Soboleva AG, *et al*. The Role of Transcription Factor PPAR-γ in the Pathogenesis of Psoriasis, Skin Cells, and Immune Cells. International Journal of Molecular Sciences. 2022; 23: 9708. https://doi.org/10.3390/ijms23179708.

[26] Kumar S, Chhimwal J, Kumar S, Singh R, Patial V, Purohit R, *et al*. Phloretin and phlorizin mitigates inflammatory stress and alleviate adipose and hepatic insulin resistance by abrogating PPARγ S273-Cdk5 interaction in type 2 diabetic mice. Life Sciences. 2023; 322: 121668. https://doi.org/10.1016/j.lfs.2023.121668.

[27] Ji X, Zhang W, Yin L, Shi Z, Luan J, Chen L, *et al*. The Potential Roles of Post-Translational Modifications of PPARγ in Treating Diabetes. Biomolecules. 2022; 12: 1832. https://doi.org/10.3390/biom12121832.

[28] Zeng S, Chen Y, Wei C, Tan L, Li C, Zhang Y, *et al*. Protective effects of polysaccharide from Artocarpus heterophyllus Lam.(jackfruit) pulp on non-alcoholic fatty liver disease in high-fat diet rats via PPAR and AMPK signaling pathways. Journal of Functional Foods. 2022; 95: 105195. https://doi.org/10.1016/j.jff.2022.105195.

[29] Qi F, Li T, Deng Q, Fan A. The impact of aerobic and anaerobic exercise interventions on the management and outcomes of non-alcoholic fatty liver disease. Physiological Research. 2024; 73: 671–686. https://doi.org/10.33549/physiolres.935244.

[30] Salih KJ, Sabir DK, Abdoul HJ. Glycolysis regulation to maintain blood glucose homeostasis. Kurdistan Journal of Applied Research. 2022; 7: 114–124. https://doi.org/10.24017/Scince.2022.1.10.

[31] Mazloomi S, Farimani MS, Tavilani H, Karimi J, Amiri I, Ab-

basi E, *et al*. Granulosa cells from immature follicles exhibit restricted glycolysis and reduced energy production: a dominant problem in polycystic ovary syndrome. Journal of Assisted Reproduction and Genetics. 2023; 40: 343–359. https://doi.org/10.1007/s10815-022-02676-w.

[32] Cao Z, Zhou Q, An J, Guo X, Jia X, Qiu Y. Glycolytic Dysfunction in Granulosa Cells and Its Contribution to Metabolic Dysfunction in Polycystic Ovary Syndrome. Drug Design, Development and Therapy. 2025; 19: 5255–5270. https://doi.org/10.2147/DDDT.S525651.

[33] Yadav D, Lee JY, Puranik N, Chauhan PS, Chavda V, Jin JO, *et al*. Modulating the Ubiquitin-Proteasome System: A Therapeutic Strategy for Autoimmune Diseases. Cells. 2022; 11: 1093. https://doi.org/10.3390/cells11071093.

[34] Li X, Yang Y, Zhang B, Lin X, Fu X, An Y, *et al*. Lactate metabolism in human health and disease. Signal Transduction and Targeted Therapy. 2022; 7: 305. https://doi.org/10.1038/s41392-022-01151-3.

[35] She F, Liu K, Anderson BW, Pisithkul T, Li Y, Fung DK, *et al*. Pyruvate kinase directly generates GTP in glycolysis, supporting growth and contributing to guanosine toxicity. mBio. 2025; 16: e0379824. https://doi.org/10.1128/mbio.03798-24.